Relationship between valence of titania and apatite mineralization behavior in simulated body environment

Journal:	*Journal of the American Ceramic Society*
Manuscript ID	JACERS-46690.R1
Manuscript Type:	Article
Date Submitted by the Author:	n/a
Complete List of Authors:	Miyazaki, Toshiki; Kyushu Kogyo Daigaku - Wakamatsu Campus, Imanaka, Satoshi Akaike, Jun
Keywords:	titanium oxide, bioactivity, calcium phosphate, apatite
Author-supplied Keyword: If there is one additional keyword you would like to include that was not on the list, please add it below::	valence

Relationship between valence of titania and apatite mineralization behavior in simulated body environment

Toshiki Miyazaki, Satoshi Imanaka, Jun Akaike

Graduate School of Life Science and Systems Engineering, Kyushu Institute of Technology, Kitakyushu, Japan

Corresponding author: Toshiki Miyazaki

Graduate School of Life Science and Systems Engineering, Kyushu Institute of Technology, 2-4, Hibikino, Wakamatsu-ku, Kitakyushu 808-0196, Japan

Tel./Fax: +81-93-695-6025

E-mail: tmiya@life.kyutech.ac.jp

Abstract

Titania-based materials are attractive for hard tissue repair due to their bone-bonding ability induced by apatite formation in the body environment. Various surface treatments have therefore been developed to produce a hydrated titania layer on Ti and its alloys. Titania takes various valences, such as TiO (Ti^{2+}) and Ti_2O_3 (Ti^{3+}), as well as typical TiO_2 (Ti^{4+}); however, there is no comprehensive study of structural effects on the apatite-forming ability of these titanias. In this study, we investigated apatite formation on titania powders with various valences in simulated body fluid. Anatase- and rutile-type TiO_2 formed apatite in simulated body fluid within 7 days, but TiO and Ti_2O_3 did not. In contrast, when the titania powders were treated with NaOH solution, the surface converted to tetravalent titania and all samples formed apatite. It is proposed that the surface electrical states of TiO and Ti_2O_3 are strongly affected by their bulk conductivity and that these behaved like pure Ti metal, which has poor apatite-forming ability. Apatite formation was favorable when the titania had a high absolute value and exhibited high fluctuations of zeta potential during initial stages in simulated body fluid, owing to adsorption of large amounts of Ca^{2+} and HPO_4^{2-}.

1. Introduction

Titanium and its alloys are light, tough, and have low cytotoxicity, so they are used as biomaterials for repairing hard tissues that operate under loaded conditions, such as dental implants and artificial joints. To be stable for use in bone tissue for a long period, it is desired to impart bone-bonding ability to these materials. Ti–OH groups on titania bind to Ca^{2+} and HPO_4^{2-} ions in the body environment, inducing deposition of bone-like apatite on its surface.[1,2] The apatite thus formed is believed to contribute to bone bonding.[3] Various kinds of surface modification of titanium metal to form titania have been attempted to provide bone-bonding ability.[4–7]

Most titanium oxides studied as biomaterials are tetravalent, such as anatase and rutile. Titanium also forms divalent and trivalent oxides. The Ti_2O_3–TiO_2 thin film obtained by ultraviolet (UV) irradiation of TiO_2, prepared by sol–gel synthesis, exhibits photocatalytic activity in response to visible light.[8] This implies the possibility for development of novel bone-bonding biomaterials that can be easily sterilized using visible light. A Ti_2O_3-based biosensor has also been developed.[9] Apatite has high affinity with various proteins, thus novel protein biosensors can be designed by the

combination of Ti_2O_3 and apatite. There is, however, no comprehensive study of the apatite-forming ability of titanias with different valences.

In this study, the apatite-forming ability of titania powders with different valences and crystalline phases was investigated in simulated body fluid (SBF). The valence dependence is discussed from the viewpoints of zeta potential, defect structure, and conductivity. The effect of NaOH treatment on apatite formation was also investigated.

2. Materials and Methods

2.1. Specimens

Divalent TiO, trivalent Ti_2O_3 (Kojundo Chemical Lab. Co., Ltd., Japan), tetravalent anatase-type TiO_2 (MC-50, average primary particle size: 24 nm; Ishihara Sangyo Kaisha Ltd., Japan, and FUJIFILM Wako Pure Chemical Co., Japan), and rutile-type TiO_2 (FUJIFILM Wako Pure Chemical Co.) were used. The particle sizes of TiO and Ti_2O_3 were relatively large (around 1 to 5 mm), so these reagents were ground in a mortar for 7 minutes prior to use.

2.2. Surface treatment

A mass of 0.1 g of each titania powder and 10 mL of 10 M NaOH (97.0% NaOH, Nacalai Tesque, Inc., Japan) aqueous solution were placed in a Teflon test tube and shaken at 60°C for 24 h using a shaking water bath (H-11, Taitec Co., Japan) operated at a shaking frequency of 120 strokes/min. After NaOH treatment, each sample was filtered, washed with ultrapure water, and dried at 40°C for 1 day.

2.3. Specific surface area measurement

Adsorption isotherms of the untreated and NaOH-treated samples were measured using an automatic specific surface area or pore distribution analyzer (BELSORP-mini II, Bell Japan Co., Ltd., Japan). The sample after NaOH treatment was heat-treated *in vacuo* at 100–150°C for 2 h. Equilibration time was 300 s and N_2 gas was adsorbed at −196°C. Under conditions where the value of the adsorption parameter C was 50–200, the specific surface area was calculated on the basis of the Brunner–Emmett–Teller (BET) theory.

2.4. Immersion in simulated body fluid

Masses of 2 g of untreated and NaOH-treated titania powder were fixed on carbon tape attached to a glass plate and immersed in SBF at 36.5°C for various periods. The SBF was prepared according to a previous report.[10] The amount of SBF was 4.7 mL per 1 m^2/g of the titania powder. After immersion, the sample was removed from solution, washed with ultrapure water for 30 min, and dried at 40°C for 1 day.

2.5. Analysis

The masses of the samples after soaking in SBF were measured by an electronic balance (CP324S, Sartorius AG, Germany). The surface structures of the titanias before and after soaking in SBF were analyzed by thin-film X-ray diffraction (TF-XRD; MXP3V, Mac Science Ltd., Japan) and scanning electron microscopy (SEM; S-3500N, Hitachi Co., Japan). For TF-XRD, the X-ray source was CuKα, the tube voltage was 40 kV, the tube current was 30 mA, and the incident angle was 1°. SEM observations were performed after vacuum vapor deposition of high-purity carbon using a carbon coater (CADE, Meiwafosis Co., Ltd., Japan).

The surface zeta potentials of the samples were measured with a zeta potential analyzer (ELS-Z, Otsuka Electronics Co., Ltd., Japan). A quartz cell was used for the measurement. The samples before and after immersion in SBF were measured in 10 mM NaCl aqueous solution and SBF, respectively.

Changes in the surface chemical state of the samples due to NaOH treatment were analyzed with an X-ray photoelectron spectroscopy analyzer (XPS; KRATOS AXIS-NOVA, Shimadzu Co., Japan). The binding energy was corrected using the C_{1s} peak (284.6 eV) of surface-contaminated hydrocarbons as a reference.

The concentration of surface OH groups on the samples before and after NaOH treatment was quantitatively measured by the zinc complex substitution method described in a previous report.[11] Briefly, after soaking the sample in a mixed solution of 2 M NH_4Cl and 0.1 M $ZnCl_2$ adjusted to pH 6.9 with aqueous NH_3 solution, the samples were transferred into 2.4 M HNO_3. The Zn concentration released into the HNO_3 was measured by inductively coupled plasma atomic emission spectroscopy (ICP–AES; ICPE-9800 Shimadzu Co., Japan). The amount of OH released was calculated from the measured Zn concentration.

3. Results

Table 1 shows the specific surface areas of the different titanias before and after NaOH treatment. The specific surface area of anatase (Ishihara) was much larger than the others because it was nanosized. The specific surface area tended to increase on NaOH treatment. This is attributed to formation of fine sodium titanate particles on the surface. In contrast, the specific surface area of anatase (Ishihara) decreased. This is probably because the effect of aggregation was more prominent than that of sodium titanate formation.

Table 2 shows the concentrations of OH groups on the different titanias before and after NaOH treatment. Before the treatment, the OH content increased in the order: anatase (Ishihara) < anatase (Wako) < rutile < TiO < Ti_2O_3. After treatment, OH content increased for all samples.

Figure 1 shows the mass change of the samples in SBF. For all samples, a mass loss of approximately 1 mg was observed after 1 day. This is probably because the sample detached from the substrate. Thereafter, the masses of rutile and anatase increased by approximately 1.5–2 mg within 7 days, but those of TiO and Ti_2O_3 hardly

increased. This mass increase is considered to be due to apatite formation.

Figure 2 shows TF-XRD patterns of the samples before and after soaking in SBF. Broad diffraction peaks attributed to low-crystalline apatite were observed for anatase and rutile after SBF immersion, but not for TiO and Ti_2O_3. In the SEM photographs shown in Fig. 3, spherical particles were observed for anatase and rutile, but only angular particles were observed for TiO and Ti_2O_3.

Figure 4 shows changes in zeta potential of the samples in SBF within 1 day. Before immersion, the rutile and anatase (Ishihara) were positively charged, while the other titanias were negatively charged. The former tended to decrease and then slightly increase, while the latter showed the opposite behavior. The fluctuation ranges within 1 day were 10 mV for TiO, 16 mV for Ti_2O_3, 25 to 37 mV for anatase, and 33 mV for rutile.

Figure 5 shows Ti_{2p} XPS spectra of TiO and Ti_2O_3 before and after NaOH treatment. Even before treatment, peaks assigned to TiO_2 and to TiO and Ti_2O_3 were observed at around 456.5 and 462.5 eV, respectively. This indicates that their surfaces were already partially oxidized by air. After treatment, the peaks assigned to TiO and

Ti_2O_3 completely disappeared, and only those assigned to TiO_2 were detected.

Figure 6 shows TF-XRD patterns of NaOH-treated samples before and after soaking in SBF. The diffraction patterns before soaking were almost the same as those without NaOH treatment, meaning that only the top surface is converted to tetravalent by the treatment. Broad peaks assigned to low-crystalline apatite were observed for all samples. SEM photographs of the samples are shown in Fig. 7. Needle-like particles larger than 10 μm and fine particles smaller than 1 μm were observed before the soaking. Morphology of the needle-like particles was similar to sodium titanate particles prepared by hydrothermal process[12]. On the other hand, spherical particles were observed for all samples after the soaking.

Figure 8 shows the correlation between the difference in zeta potential within 1 day and the mass change from 1 to 7 days for each sample. The larger the zeta potential difference, the larger was the mass change. The correlation coefficient was calculated to be 0.891, indicating that there is a strong correlation between these parameters.

Discussion

The apatite-forming ability of titania was found to significantly decrease with decreasing valence (Figs. 1 to 3). Low-valence TiO and Ti_2O_3 did not form apatite, although they contained larger amounts of Ti–OH groups than rutile and anatase (Table 2). It has been reported that the apatite-forming ability of rutile and anatase layers formed by anodic oxidation is enhanced with increase in amount of surface Ti-OH group[13]. Therefore, these suggests that Ti–OH groups on low-valence titanias have poor apatite-forming ability. This assumption is also supported by the fact that when TiO and Ti_2O_3 were initially treated with NaOH solution, the surface titania became tetravalent and the apatite-forming ability was significantly enhanced (Figs. 6 and 7). It is considered that TiO and Ti_2O_3 were oxidized as follows by NaOH treatment:

$$TiO + H_2O \rightarrow TiO_2 + H_2; \quad (1)$$

$$Ti_2O_3 + H_2O \rightarrow 2TiO_2 + H_2. \quad (2)$$

Vacuum heating of NaOH-treated Ti metal reportedly produced low-valence suboxides and lost apatite-forming ability,[14] which is a similar tendency to that of the present results. Although the surface of NaOH-treated TiO is almost covered by the apatite particles, intensity of TF-XRD patterns of the apatite was smaller than the other

NaOH-treated titanias (Figs. 6 and 7). Ca/Ti and P/Ti atomic ratios of the surface of NaOH-treated TiO were around 11 and 5, respectively, smaller than the other titanias (Ca/Ti; 26–54, P/Ti; 14–27). Therefore, it is assumed that the thickness of the apatite layer formed on NaOH-treated TiO is smaller than the other titanias.

Why do low-valence titanias exhibit poor apatite-forming ability? Hanawa *et al.* precisely investigated the formation behavior of calcium phosphate in Hanks' solution on pure Ti metal surface by XPS.[15] Calcium phosphate formed on Ti metal, but its thickness was only 6.4 nm after 1 day. In this state, it is considered that the calcium phosphate is electronically affected by the substrate composed of titania and Ti metal, but not affected in terms of ionic field.[16] It is also reported that the passive film on the Ti metal surface was mainly composed of TiO_2, but its thickness was only 4 nm. It is assumed that titania in the passive film may also be electronically affected by the Ti metal substrate, similar to that of deposited calcium phosphate. Therefore, the ability of this titania to form apatite is extremely poor compared with that of a TiO_2 layer prepared by sol–gel synthesis or anodic oxidation.[2,6] Furthermore, TiO_2 has semiconductor characteristics, while TiO and Ti_2O_3 are conductive.[17] It is therefore

assumed that the surfaces of TiO and Ti_2O_3 are electronically affected by the conductivity of the respective bulk titanias and behave similarly to pure Ti metal, resulting in poor apatite formation.

The effects of vacancy formation can also be a factor governing apatite formation. O vacancies are reported to favor apatite formation on various titania surfaces; for example, when an anatase or rutile surface is irradiated by UV light, a mixed surface of Ti^{4+} and Ti^{3+} with O vacancies is created by reduction, which improves apatite formation in SBF.[18–20] This is because the O vacancies that are created with Ti^{3+} react with the surrounding water to form Ti–OH groups. Hashimoto *et al.* investigated the apatite-forming ability of Ti metal heated in N_2–O_2 mixed gas with controlled O_2 partial pressure, and showed that apatite formation was enhanced by a decrease in O_2 partial pressure.[21] This is because O vacancies formed by the heat treatment reacted with water to give OH radicals that were able to adsorb Ca^{2+} and HPO_4^{2-}. When TiO_2 is added to a Ti_2O_3 matrix, not only O vacancies, but also Ti vacancies, are formed by the following reaction:

$$3TiO_2 \rightarrow 3Ti_{Ti}^{\cdot} + 6O_O^X + V_{Ti}^{''''} \qquad (3)$$

First-principle calculations suggest that coexistence of O and Ti vacancies in Ti_2O_3 crystals causes vacancy formation to be energy-negative and therefore thermodynamically stable.[22] Cations such as Ca^{2+} are considered to be easily adsorbed on negatively charged Ti vacancies. The measured Ca and P contents on the present Ti_2O_3 surface after soaking in SBF for 1 day were 0.3% and 0.05%, respectively, indicating that Ca was more favorably adsorbed than P. However, the formed Ca-titania complex would have poor apatite-forming ability. Ca contents on the present TiO and Ti_2O_3 were below 0.5% and 0.2%, respectively, even after soaking in SBF for 7 days. It is documented that large amounts of Ca^{2+} and HPO_4^{2-} are adsorbed in the initial stage of apatite nucleation on the surfaces of both NaOH- and heat-treated Ti.[23] However, in the case of the present TiO and Ti_2O_3, such a state did not occur because Ca^{2+} adsorption was saturated.

Apatite formation is also governed by changes in zeta potential. Anatase generally shows a negative zeta potential under neutral conditions,[24] but the present anatase (Ishihara) showed a positive potential. The presence of S was confirmed by XPS in anatase (Ishihara), so this difference is attributed to deposits formed during

manufacturing. The zeta potential rose and then fell within 1 day, or vice versa, for all samples. This is considered to be due to adsorption of Ca^{2+} and HPO_4^{2-} in SBF that occurred with some time lag. The initial zeta potentials of the anatase and rutile that formed apatite had absolute values of approximately 25–35 mV. Hashimoto *et al.* investigated apatite formation on Ti heated under various conditions in N_2–O_2 mixed gas with an O_2 partial pressure of 10^{-14} Pa.[25] In this case, apatite coverage in SBF exceeded 50% when the zeta potential on the Ti surface was 10 to 20 mV or −30 to −25 mV. The titania used in this study also exhibited this tendency. Samples with larger fluctuations in zeta potential were more likely to form apatite in SBF. This is attributed to the adsorption of large amounts of Ca^{2+} and HPO_4^{2-} that enhance apatite nucleation.

Reported initial zeta potentials of NaOH- and heat-treated Ti were approximately −10 mV[26] and the fluctuation range was approximately 15 mV,[27] which are smaller than the values for the present titania powder. However, in the case of the previous study, the elution of Na^+ from sodium titanate on the surface created many Ti–OH groups and increased the pH of the surrounding fluid, leading to acceleration of apatite formation. Therefore, it is suggested that leached and unleached titanias have different surface

potential characteristics that are favorable for apatite formation.

Conclusions

Apatite-forming ability of titania with different valences was investigated in SBF. It was found that the apatite-forming abilities of TiO and Ti_2O_3 were much lower than that of TiO_2. Conductivity and vacancy state of low-valence titanias may affect the surface properties to inhibit apatite formation. Absolute values and fluctuation ranges of the zeta potential during the initial stage in SBF also govern apatite formation. The findings in this study may contribute to establishment of general principles for apatite formation on metal oxides in the body environment.

Acknowledgment

We thank Kathryn Sole, PhD, from Edanz Group (https://en-author-services.edanzgroup.com/ac) for editing a draft of this manuscript.

References

1. Li P, Ohtsuki C, Kokubo T, Nakanishi K, Soga N, de Groot K. The role of hydrated

silica, titania, and alumina in inducing apatite on implants. J Biomed Mater Res. 1994;28(1):7-15.

2. Uchida M, Kim HM, Kokubo T, Fujibayashi S, Nakamura T. Structural dependence of apatite formation on titania gels in a simulated body fluid. J Biomed Mater Res A. 2003;64(1):164-170.

3. Yan WQ, Nakamura T, Kobayashi M, Kim HM, Miyaji F, Kokubo T. Bonding of chemically treated titanium implants to bone. J Biomed Mater Res. 1997;37(2):267-275.

4. Kim HM, Miyaji F, Kokubo T, Nakamura T. Preparation of bioactive Ti and its alloys via simple chemical surface treatment. J Biomed Mater Res. 1996;32(3):409-417.

5. Wang XX, Hayakawa S, Tsuru K, Osaka A. A comparative study of in vitro apatite deposition on heat-, H_2O_2-, and NaOH-treated titanium surfaces. J Biomed Mater Res. 2001;54(2):172-178.

6. Yang BC, Uchida M, Kim HM, Zhang X, Kokubo T. Preparation of bioactive titanium metal via anodic oxidation treatment. Biomaterials.

2004;25(6):1003-1010.

7. Sugino A, Tsuru K, Hayakawa S, Kikuta K, Kawachi G, Osaka A, et al. Induced deposition of bone-like hydroxyapatite on thermally oxidized titanium substrates using a spatial gap in a solution that mimics a body fluid. J Ceram Soc Japan. 2009;117(4):515-520.

8. Liu H, Yang W, Ma Y, Yao J. Extended visible light response of binary TiO_2-Ti_2O_3 photocatalyst prepared by a photo-assisted sol–gel method. Appl Catal A. 2006;299:218-223.

9. Nazeran H, Macrow JD, Pilowski P. Development of a low cost microP-based blood gas monitor. Australas Phys Eng Sci Med. 1995;18(3):143-145.

10. Cho SB, Kokubo T, Nakanishi K, Soga N, Ohtsuki C, Nakamura T, et al. Dependence of Apatite Formation on Silica Gel on Its Structure: Effect of Heat Treatment. J Am Ceram Soc. 1995;78(7):1769-1774.

11. Sakamoto H, Hirohashi Y, Saito H, Doi H, Tsutsumi Y, Suzuki Y, et al. Effect of Active Hydroxyl Groups on the Interfacial Bond Strength of Titanium with Segmented Polyurethane through γ-mercapto Propyl Trimethoxysilane. Dent Mater

J. 2008;27(1):81-92.

12. Kondo Y, Goto T, Sekino T. Sorption capacity of seaweed-like sodium titanate mats for Co^{2+} removal. RSC Adv. 2020;10(67):41032-41040.

13. Zhao Y, Xiong T, Huang W. Effect of heat treatment on bioactivity of anodic titania films. Appl. Surf. Sci. 2010;256(10):3073-3076.

14. Ravelingien M, Mullens S, Luyten J, Meynen V, Vinck E, Vervaet C, et al. Thermal decomposition of bioactive sodium titanate surfaces. Appl Surf Sci. 2009;255(23):9539-9542.

15. Hanawa T, Ota M. Calcium phosphate naturally formed on titanium in electrolyte solution. Biomaterials. 1991;12(8):767-774.

16. Sato N. Critical issues on passivity. Bull Jpn Inst Met. 1985;24(9):724-726 (in Japanese).

17. Xu B, Sohn HY, Mohassab Y, Lan Y. Structures, preparation and applications of titanium suboxides. RSC Adv. 2016;6(83):79706-79722.

18. Liu X, Zhao X, Ding C, Chu PK. Light-induced bioactive TiO_2 surface. Appl Phys Lett. 2006;88(1):013905.

19. Han Y, Chen D, Sun J, Zhang Y, Xu K. UV-enhanced bioactivity and cell response of micro-arcoxidized titania coatings. Acta Biomater. 2008;4(5):1518-1529.

20. Shozui T, Tsuru K, Hayakawa S, Osaka A. Enhancement of in vitro apatite-forming ability of thermally oxidized titanium surfaces by ultraviolet irradiation. J Ceram Soc Japan. 2008;116(4):530-535.

21. Hashimoto M, Hayashi K, Kitaoka S. Enhanced apatite formation on Ti metal heated in P_{O2}-controlled nitrogen atmosphere. Mater. Sci. Eng. C. 2013;33(7):4155-4159.

22. Pan Y, Li YQ, Zheng QH, Xu Y. Point defect of titanium sesquioxide Ti_2O_3 as the application of next generation Li-ion batteries. J Alloys Compd. 2019;786:621-626.

23. Takadama H, Kim HM, Kokubo T, Nakamura T. TEM-EDX study of mechanism of bonelike apatite formation on bioactive titanium metal in simulated body fluid. J Biomed Mater Res. 2001;57(3):441-448.

24. Parks GA. The isoelectric points of solid oxides, solid hydroxides, and aqueous hydroxo complex systems. Chem Rev. 1965;65(2):177-198.

25. Hashimoto M, Ogawa T, Kitaoka S, Muto S, Furuya M, Kanetaka H, et al. Control

of surface potential and hydroxyapatite formation on TiO_2 scales containing nitrogen-related defects. Acta Mater. 2018;155:379-385.

26. Pattanayak DK, Yamaguchi S, Matsushita T, Nakamura T, Kokubo T. Apatite-forming ability of titanium in terms of pH of the exposed solution. J R Soc Interface. 2012;9(74):2145-2155.

27. Kim HM, Himeno T, Kawashita M, Lee JH, Kokubo T, Nakamura T. Surface potential change in bioactive titanium metal during the process of apatite formation in simulated body fluid. J Biomed Mater Res A. 2003;67(4):1305-1309.

Table 1. Specific surface areas of different titanias before and after NaOH treatment

Sample	Specific surface area / $m^2 \cdot g^{-1}$	
	Before NaOH treatment	After NaOH treatment
TiO	1.04	2.22
Ti_2O_3	0.861	5.55
Anatase (Ishihara)	65.4	23.9
Anatase (Wako)	10.2	12.8
Rutile	6.34	6.55

Table 2. Concentrations of OH groups on different titanias before and after NaOH treatment

Sample	Amount / $10^{19}\cdot m^{-2}$	
	Before NaOH treatment	After NaOH treatment
TiO	6.04	26
Ti_2O_3	6.76	9.79
Anatase (Ishihara)	2.82	5.36
Anatase (Wako)	3.25	3.37
Rutile	3.27	4.27

Figure captions

Figure 1. Change in mass of titania samples after soaking in simulated body fluid.

Figure 2. Thin-film X-ray diffraction patterns of surfaces of samples before and after soaking in simulated body fluid for 7 days.

Figure 3. Scanning electron micrographs of surfaces of samples after soaking in simulated body fluid for 7 days.

Figure 4. Change in zeta potential of samples after soaking in simulated body fluid within 1 day ($n = 3$).

Figure 5. X-ray photoelectron spectra of TiO and Ti_2O_3 before and after NaOH treatment.

Figure 6. Thin-film X-ray diffraction patterns of surfaces of NaOH-treated samples before and after soaking in simulated body fluid for 7 days.

Figure 7. Scanning electron micrographs of surfaces of NaOH-treated samples before and after soaking in simulated body fluid for 7 days.

Figure 8. Relationship between mass change from 1 to 7 days and difference in zeta potential of titania samples after soaking in simulated body fluid within 1 day. Open

circles and closed squares indicate samples with and without apatite formation in the medium, respectively.

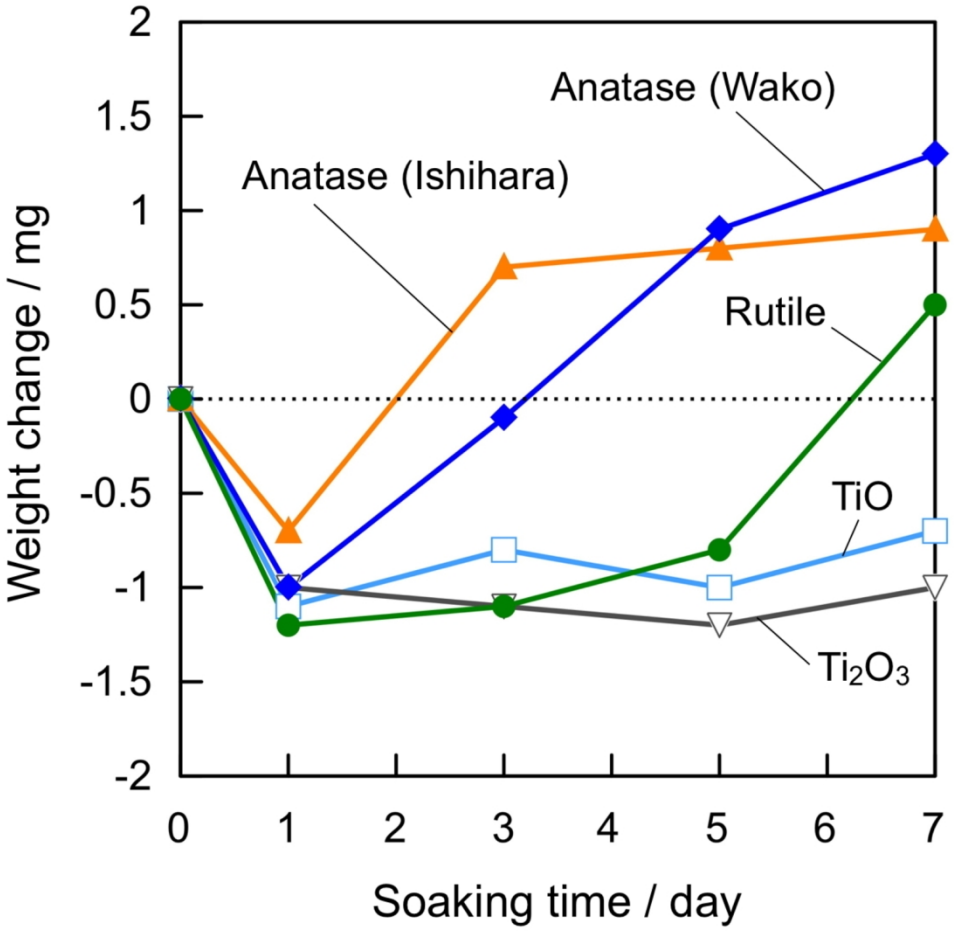

Fig.1

70x68mm (600 x 600 DPI)

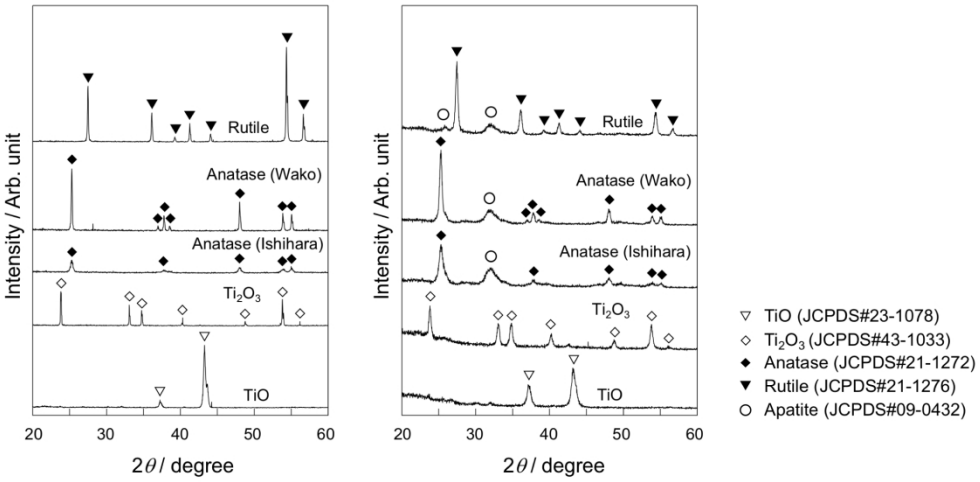

Fig.2

98x49mm (600 x 600 DPI)

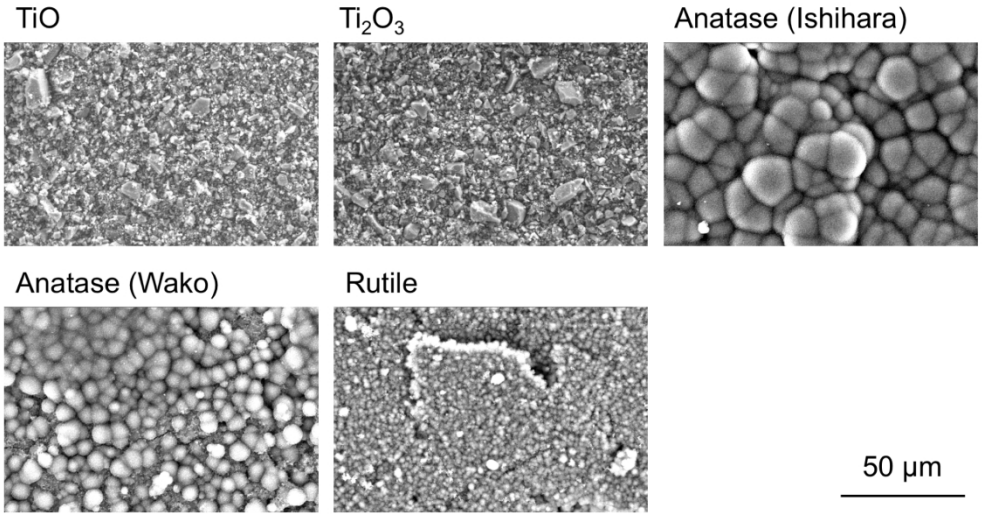

Fig.3

96x50mm (600 x 600 DPI)

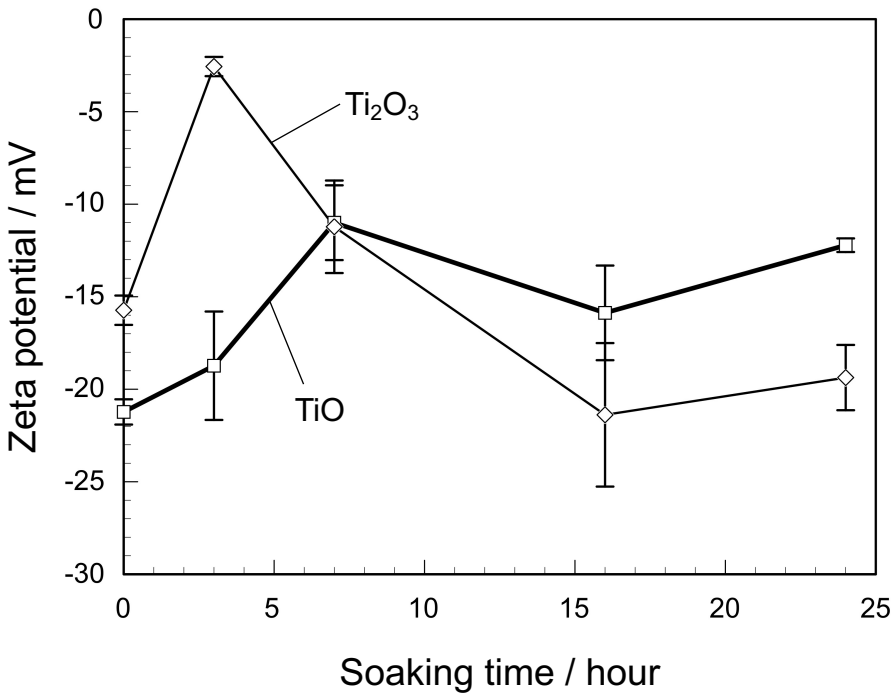
Zeta potential / mV
Soaking time / hour
Ti_2O_3
TiO
0
-5
-10
-15
-20
-25
-30
0
5
10
15
20
25

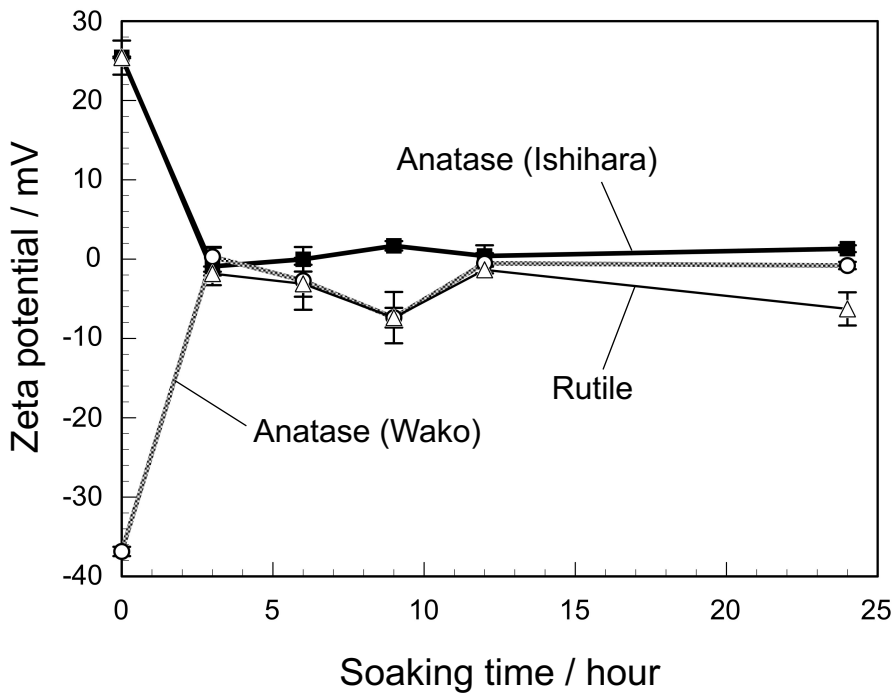
Zeta potential / mV
Soaking time / hour
Anatase (Ishihara)
Rutile
Anatase (Wako)
30
20
10
0
-10
-20
-30
-40
0
5
10
15
20
25

Fig. 4

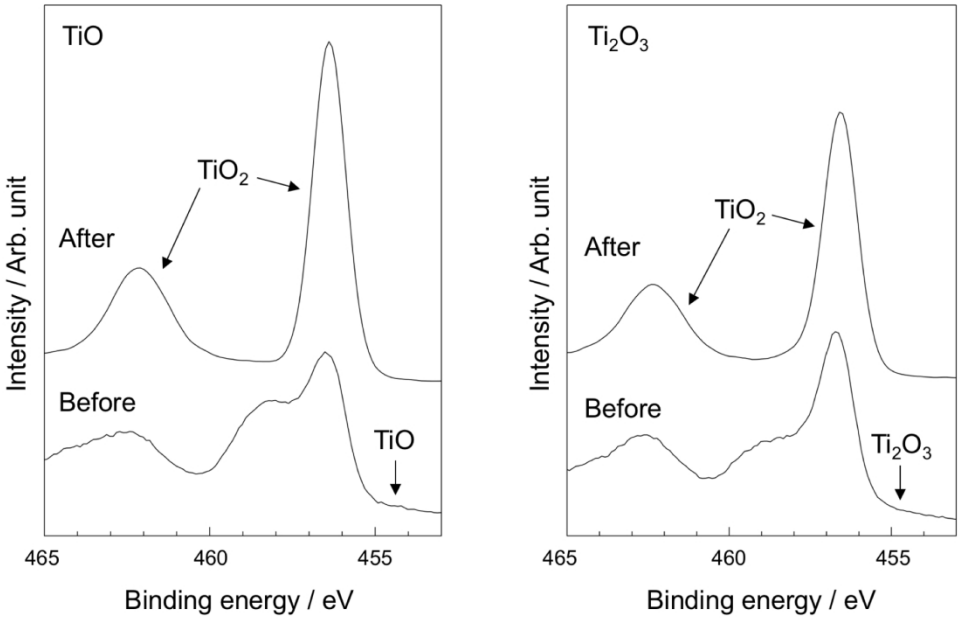

Fig.5

88x57mm (600 x 600 DPI)

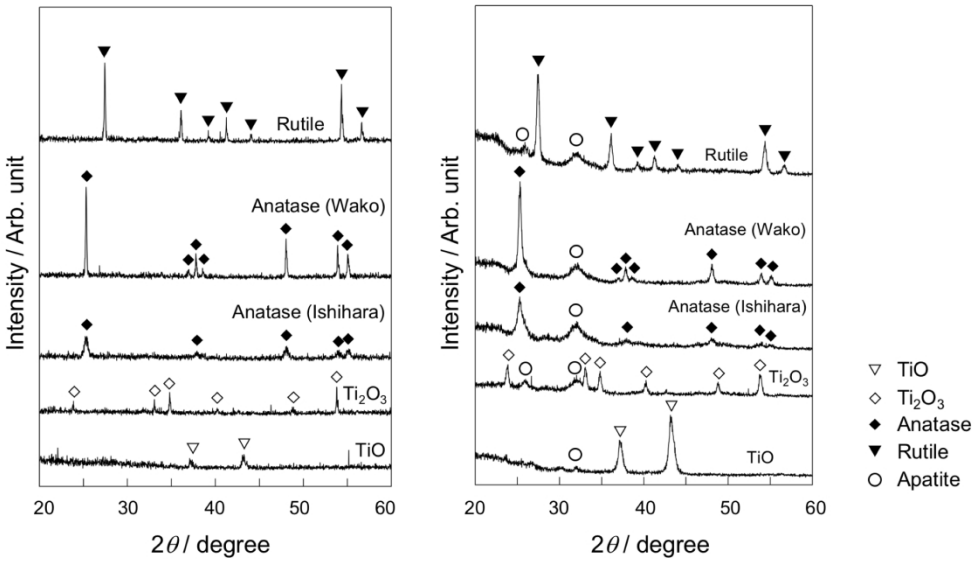

Fig.6

94x55mm (600 x 600 DPI)

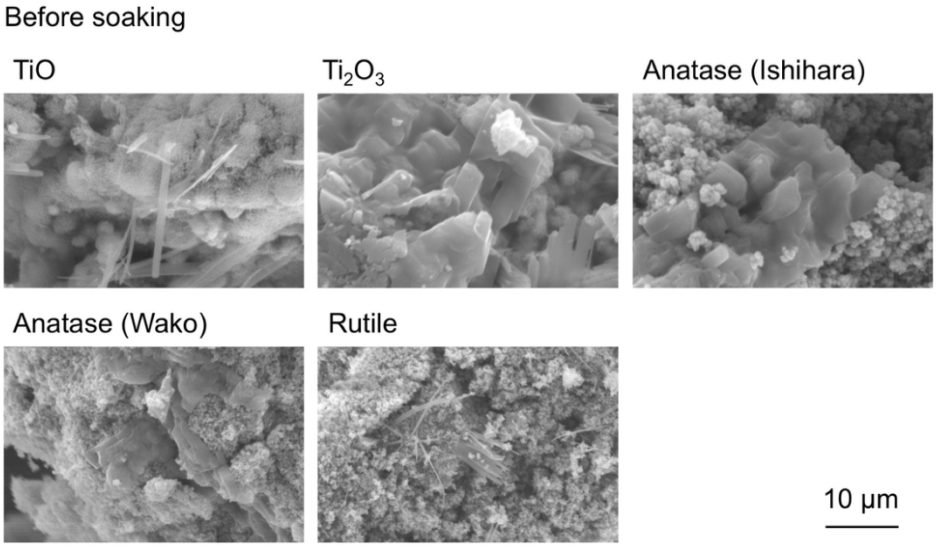

Fig. 7

Fig.7_1

99x71mm (300 x 300 DPI)

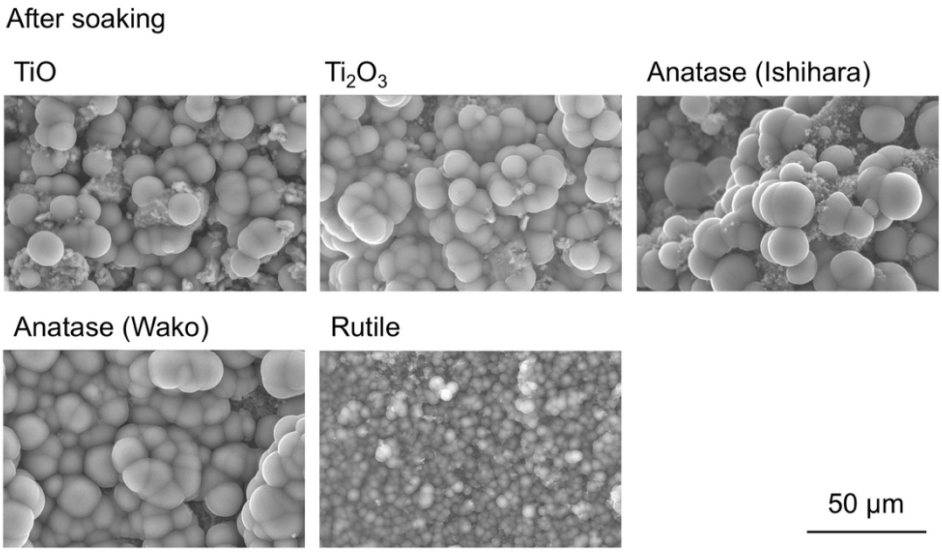

Fig. 7 (Continued)

Fig.7_2

99x71mm (300 x 300 DPI)

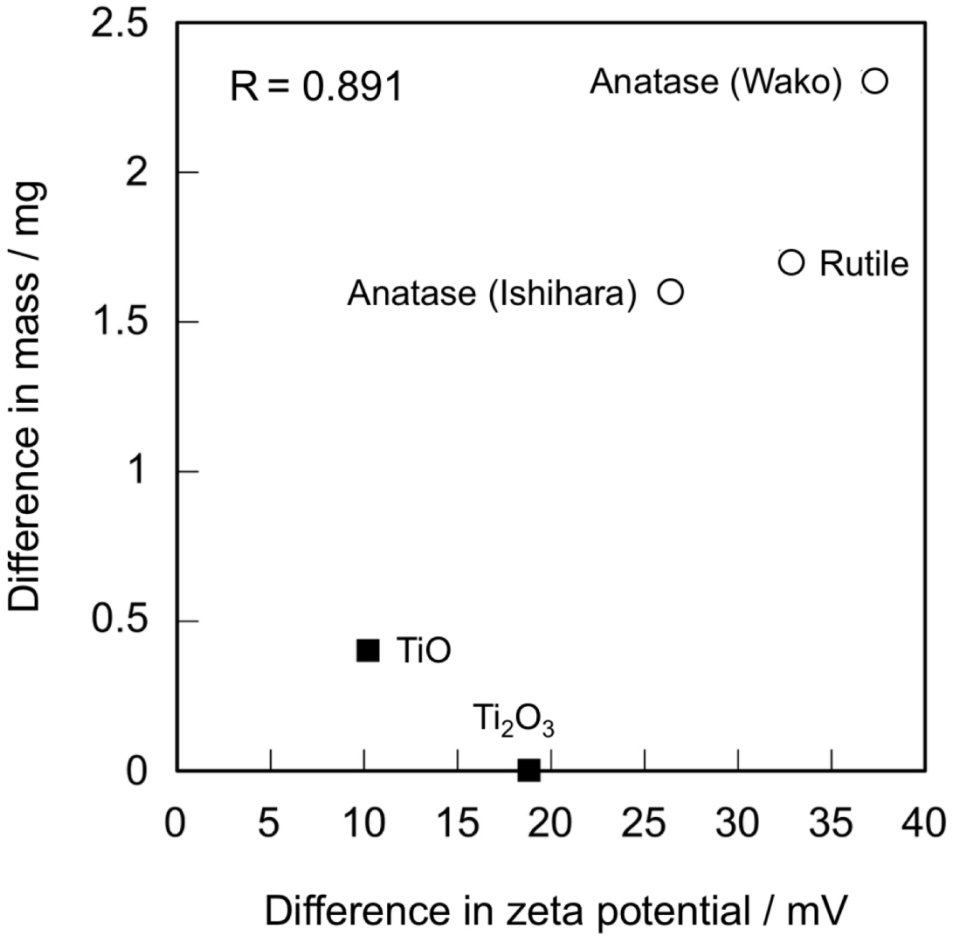

Fig.8

64x63mm (600 x 600 DPI)

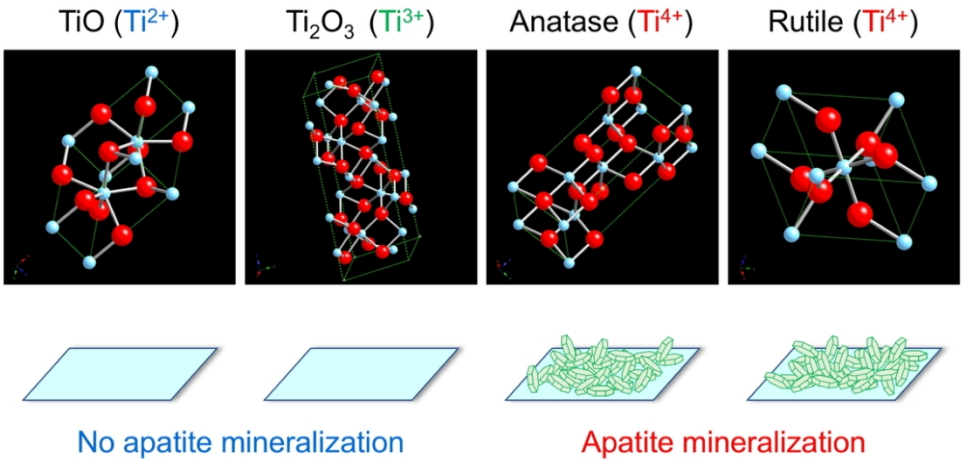

Graphical abstract

99x49mm (300 x 300 DPI)